Materials Compatibility Issues in LTCC Technology and Their Effects on Structural and Electrical Properties

H. Birol, T. Maeder and P. Ryser
Ecole Polytechnique Fédérale de Lausanne (EPFL)
Laboratoire de Production Microtechnique (LPM)
CH-1015 Lausanne, Switzerland
Tel: ++41 21 693 77 58, Fax: ++41 21 693 38 91, E-mail: hansu.birol@epfl.ch

Abstract

Although LTCC (low temperature co-fired ceramics) technology is an attractive solution for smart-packaging of micro-electronic devices, numerous studies are still underway to overcome the difficulties encountered during processing and application. These difficulties center on chemical and physical issues occurring between the LTCC components during firing. The chemical issues arise from the interaction of the glass phase(s) in the tape and the thick-films, whereas the physical issues are usually due to the shrinkage-mismatch of the tape and the screen-printed pastes. This is observed both microscopically and macroscopically in form of either chemical diffusion (by microscopy and spectroscopy analysis) or deformed structures (warpage, delamination, curling etc) respectively. The objective of this study is the basic understanding of the effects of processing conditions on the properties of the commercial thick-films those are screen-printed and fired with the LTCC tape. This will be analyzed by measuring the TCR (temperature coefficient of resistance) and sheet resistance values of PTC (positive temperature coefficient) resistors, which are prepared at different conditions. Moreover the results of a recent study, which aims to match the shrinkage behavior of the conductor pastes to that of the LTCC tape, are demonstrated.

Keywords: LTCC, co-firing, differential shrinkage, microstructure, positive temperature coefficient,

Introduction

LTCC technology, which is based on LTCC sheets of various thicknesses, offers numerous advantages for multi-disciplinary areas in various ways[1-9]. In high frequency applications, it is a stable dielectric substrate that can be co-fired (<900°C) with highly conducting Au and Ag thick-film pastes providing very low losses. On the other hand it is a mechanically and chemically stable, hermetic multi-layer media for realization of 3-D devices combining mechanical, fluidic and electrical functions in one system, which makes it attractive for sensor applications[10-17].

Among all advantages it offers, integration of thick-film pastes as conductive tracks and passive electronic components into/onto the tapes by screen-printing forms the cornerstone of this technology. High functionality can be obtained by multi-layering these printed layers, where the communication between them is enabled by vias. There is a wide range of metallurgies for the low-resistivity conductors such as Ag, Pd, Ag/Pd, Pt, Cu, etc. The cost and the application aspects are the major factors to make a selection among them. On the other hand the resistors are generally powders of ruthenium-based conducting oxides[18] such as ruthenium oxide, lead ruthenate or bismuth ruthenate, which are surrounded by a glass matrix[19]. Additionally, glass is also widely used in some conductors (fritted conductors) and in the LTCC tape. Thus most components contain a glassy phase. Common to all components, it reduces the sintering temperature. In case of resistors, it determines the resistivity by separating the conducting particles, whereas it increases adhesion to the substrate and the dielectric strength in the conductor and the tape respectively.

However, these glass phases are often dissimilar in chemistry and temperature behavior (viscosity, glass-transition temperature - T_g), which may lead to physical and chemical materials compatibility issues, such as interdiffusion /interaction and differential shrinkage.

The motivation of this paper is the basic understanding of the influence of processing parameters on the LTCC structures co-fired with PTC resistors: their effects are analyzed and solutions are proposed in order to control and avoid the problems encountered. The methods of analysis are dilatometry, scanning electron microscopy (SEM) and energy dispersive X-ray analysis (EDXS).

Preparation of samples

The samples were prepared according to the test pattern shown in figure 1. As can be seen from the figure, it consists of different resistor geometries, which is ideal to study the electrical properties as a function of the resistor length. Thus, the selected thick-film materials (table 1) were screen-printed either on (surface) or within (buried) the LTCC layers according to this layout.

The layout	Number of resistors	width / length (width=1.5 for all)
	5	1
	1	5
	1	2.5
	1	1.5
	1	0.3

Figure 1. Test pattern for electrical measurements using PTC resistors. Long rectangle in the middle represents the resistor.

Buried samples were prepared by uni-axial lamination of the screen-printed layer with a blank layer having openings at the contact points (squares on the edge) at 70°C and under 55MPa. This was followed by firing the surface-printed and buried samples. Although both cases are termed as co-firing, we would rather call the former one as co-firing for convenience and the latter as buried.

Table 1. Materials used for the test patterns

Function	Product	Specification
Substrate	Du Pont **(DP)** 951-AX LTCC	Glass-ceramic/ Ca-Al-Si-O
Resistor	ESL 2612	PTC resistor/ Ru-based
Conductor	DP 9473	Classical / Ag/Pd
	DP 5744	Classical / Au
	ESL 8837	Organometallic/Au

Firing was carried according to a 2-step profile in an LTCC-oven (ATV-PEO 601) in air atmosphere. Heating rate of 5°C/min was applied until the first dwell time of 120 minutes at 440°C, which was followed by keeping the same rate until the peak dwell time of 25 minutes at 850, 875 and 900°C separately. Finally 3 conductor-resistor pairs were prepared in two processing variants as co-fired and buried.

Four-wire electrical resistance measurements were performed by a Keithley 2000 and 7000 series multimeter and scanner respectively, while a Pt-1000 PTC resistor recorded the temperature. Sheet resistance (SR) was measured at 30, 65 and 100°C and the TCR and standard deviation (SD) was calculated according to

$$TCR = (R_{100} - R_{30}) / R_{30} (T_{100} - T_{30})$$

$$SD = \sqrt{\frac{n\sum y^2 - \left(\sum y\right)}{n(n-1)}}$$

where R is the resistance at temperature T and n is the number of values (SR or TCR) measured. It should be remembered that the geometry yielding one for the length to width ratio (width=length) is used to present the TCR and SR versus processing conditions data (figure 2), as it corresponds to 5 nominally equivalent resistors, which gives sufficient statistical information.

The dilatometry analysis was carried out on thick-film pellets. This was made by separating the organics of the pastes in acetone by applying ultrasound and drying the mixture up to 250°C gradually. The dried product was then crushed in a mortar to prepare the powders. Obtained powders were uni-axially pressed under 25MPa for 5 minutes. The pellets were then placed into the dilatometer (Setaram), which was operated by the same firing profile described for that of test patterns.

Micro-structural and EDXS analysis were performed using SEM (Philips XLF-30), which is simultaneously operated with an EDXS detector. The cross-sectional areas of both the pellets of single components and the multilayers (tape-conductor-resistor interface) were prepared using diamond films of various thicknesses (from 30 to 0.1µm). The analysis with the pellets of single components was used as a reference, to explain the material interaction in the multilayer.

The prepared surfaces were then electroded with carbon, which is the optimum alternative concerning the Au conductors used in this study. The images were taken in back-scattered electron (BSE) mode at 20keV. On the other hand the oxygen percentage was calculated by stoichiometry after the atomic percentages of the other elements are normalized to 100.

Results and discussions

1. TCR and sheet resistance

TCR and SR values are presented in figures 2 and 3 respectively, where SD is shown at the tip of the columns. One can see the firing temperatures as a series of 850, 875 and 900°C directly under the columns and the 2 processing variants (co-fired and buried) in the x-axis. On the other hand, the y-axis presents the TCR (figure 2) and SR (figure 3) values. Each triple column in one processing variant represents a commercial thick-film conductor that is fired with the PTC resistor (same resistor for all conductors).

It is evident from figure 2 that the buried samples demonstrate a high deviation than the specified TCR range, which is illustrated with red spots around 2400ppm/K (a value corresponding to the alumina substrate that is fired at 850°C for 10 minutes with an overall firing period of 45 minutes). Moreover SD reaches to extremely high values, indicating a considerable amount of unreliability.

On the other hand, the dependence of TCR on the selected conductors for co-fired samples is negligible. Although the values do not exactly match the specified range, they are close to it, with small standard deviation.

The irreproducibility and unreliability of the buried samples can be best seen in figure 3, where SR can be. an order of magnitude higher compared to the specified SR of 100ohm/square. As a result of this, SR of the buried samples is represented on a seperate y-axis on the right hand side of the co-fired samples for convenience.

It can also be seen from the figure that the SR of the co-fired samples varies among each other for different conductors, which may be attributed to their different metallurgy and glass phase composition. This will be discussed in the following sections in more detail.

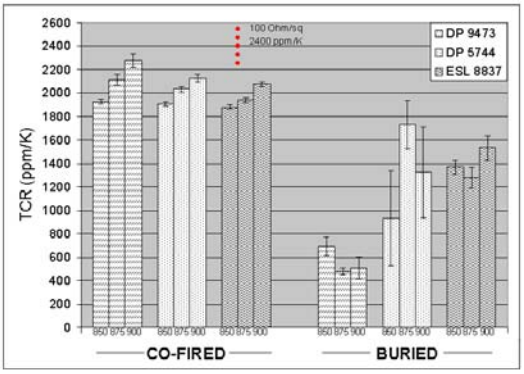

Figure 2. TCR versus processing parameters. Buried samples show a strong deviation from the expected values (shown in red spots).

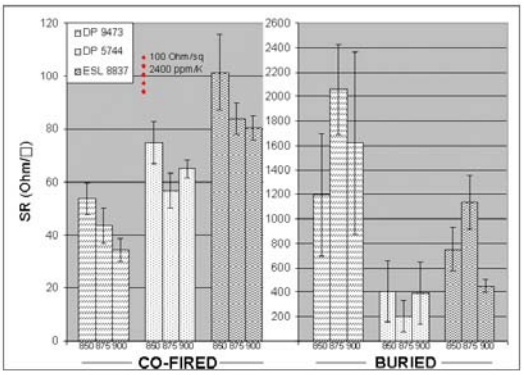

Figure 3. SR versus processing parameters. SR of buried samples are presented on the second y-axis on the right-hand side of the co-fired samples.

The presented data for buried samples in figures 2 and 3 were selected from a broad range of values, which was varying from very low to very high. Thus the reasons behind this result will receive the major attention in the following sections.

2. Chemical Issues

The chemical interactions between the co-fired components[20-22] arise from different sources. From a specific point of view, these are due to the constituents - especially the glass phase in their compositions - and also diffusion of some species, both of which are directly effected by the processing conditions[23-25].

In this paper, this is investigated by analyzing the relation between the TCR and SR values of the co-fired (surface) samples and the resistor length, which is cited to be a classical approach to check the existence of conductor – resistor chemical reactions[26]. Figure 4 shows this relation for the different conductors, which are fired at 850, 875 and 900°C. Au conductors exhibit an expected stability of TCR with varying resistor length, whereas Ag/Pd shows visible change. This variation between two metallurgies is also observed in SR versus resistor length relation. It is seen from the figure (graphs in the second row) that the samples co-fired with Ag/Pd composition has a SR value that is less than the Au conductors and it shows a relatively higher change upon changing resistor length. Among all, samples co-fired with ESL 8837 conductor seem to be the most stable conductor that is closest to the specified SR value of 100 ohm/□.

These results point a chemical interaction between the Ag/Pd conductor and the resistor, which is stronger than for Au conductors. Thus we focused our attention to the chemical composition of the conductors in order to reveal the origin of this difference between the Ag/Pd and the Au conductors using SEM and EDXS. One must note that screen printing effects (thickness increase near the terminations) also influence SR.

The SEM images, which belong to the pellets of individual conductors, are demonstrated in figure 5. It is seen from the images that all the conductors contain two major phases, the ratio of which differs significantly. This is clearly observed in the case of the Ag/Pd conductor (the first picture). Its microstructure shows large, solidified melt regions spreading out in the matrix phase, which is typical feature of a glassy phase. It is confirmed by the EDXS analysis that it is Bi-Zn-Si-rich glass, whereas the matrix is the Ag/Pd phase at 76/24 atomic ratio. The distribution of both phases is very uniform in the overall structure.

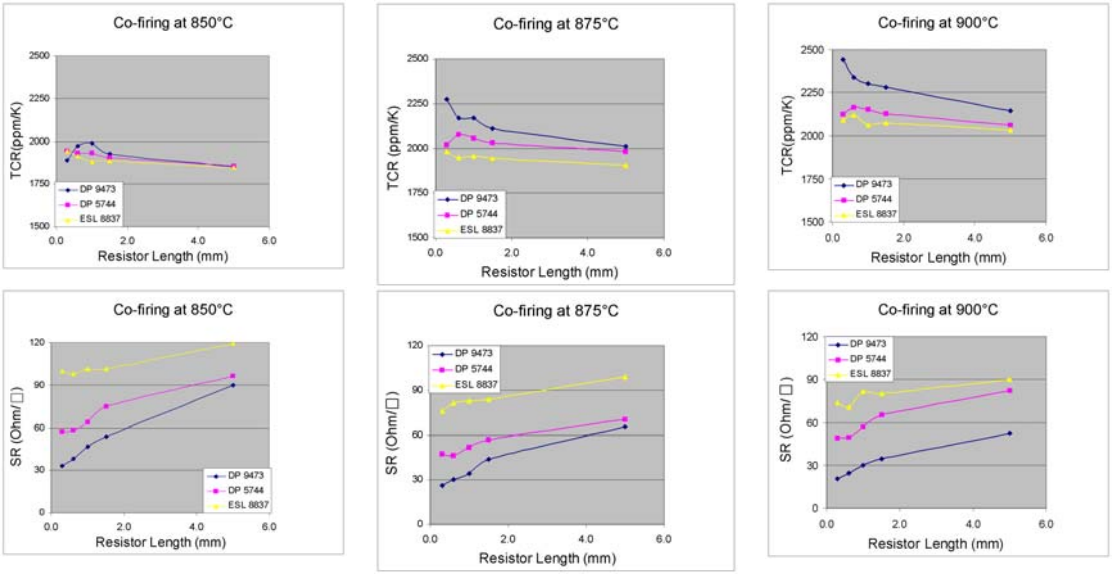

Figure 4. TCR (first row) and SR versus resistor length relation between the conductors fired at 850, 875 and 900°C.

The second and third pictures correspond to the Au conductors (DP 5744 and ESL 8837 respectively). One can observe local scratches on the surfaces, which are due to the softness of Au making it harder to prepare. Both conductors are composed of 2 major phases similar to the Ag/Pd. However in this case the matrix (Au) covers the largest area in the structure and only a limited portion is formed by the glass phase (large, black particles). Thus the ratio of the matrix to the glass is quite large. In the former one the glass is based on Bi-Pb-Si system whereas it is Pb-Si-Zn in the latter one. It is also observed that the size and distribution of the glass particles are random in both conductors. According to our understanding in light of these microstructures, the glass in the Au conductors is mainly used for adhesion to the substrate. This differs from the fritted-Ag/Pd conductor, where a much larger amount of glass also strongly aids densification. For a better understanding, the elemental analysis of the glass content of the thick-film materials and LTCC tape is presented in figure 6. It is clearly seen that Si-Pb-Zn and partially Bi are the main elements used to form the glass phase.

In light of these results (figures 4-6), further SEM and EDXS analysis were performed on the cross-section of the conductor-resistor-tape interface. The focus was made on the Ag/Pd and Au (DP 9473) conductors those co-fired with PTC resistor (figure 7).

The first microstructure, which shows 4 different regions, belongs to the sample co-fired with the Ag/Pd conductor. One can see the resistor, the conductor (white), a reaction zone denoted by RZ (light grey area with black, needle-like particles) and the LTCC substrate. Among all, RZ and conductor are the most interesting features of this microstructure.

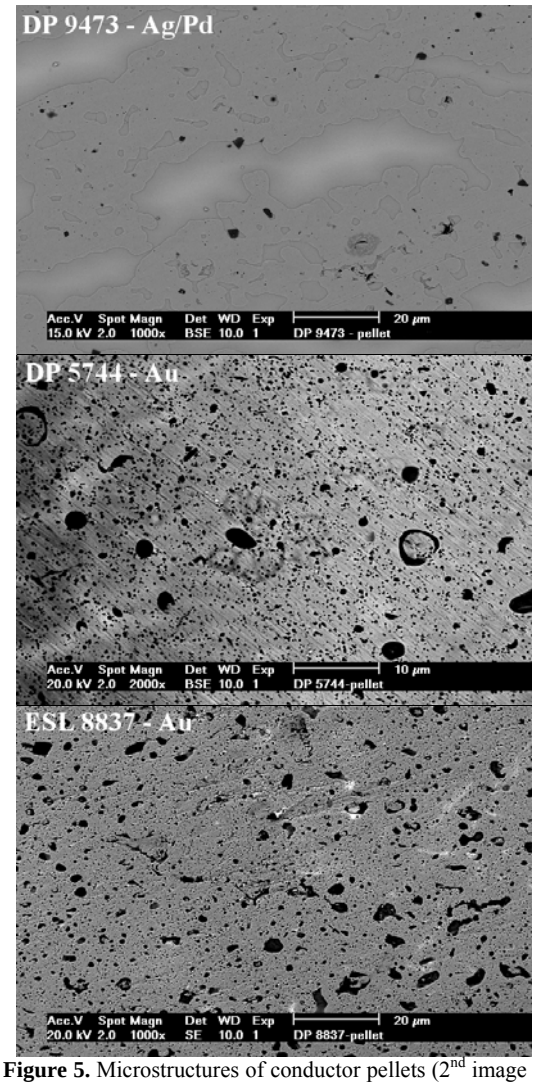

Figure 5. Microstructures of conductor pellets (2nd image is at a different magnification than the others).

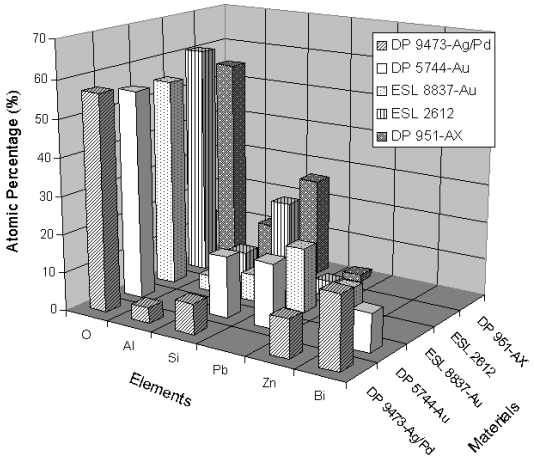

Figure 6. EDXS analysis of the glass phase of thick-film material and LTCC tape. Note that only elements those exceeding a certain limit are shown.

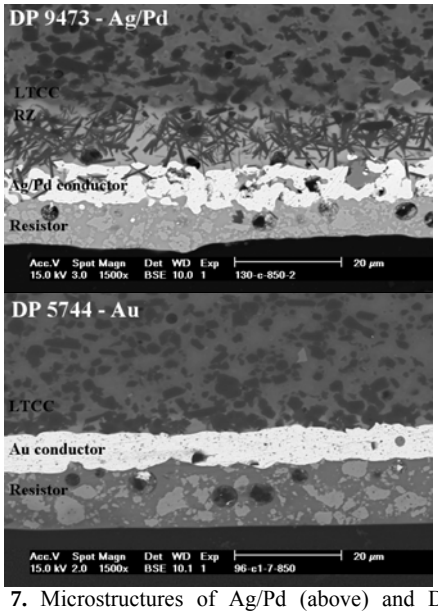

Figure 7. Microstructures of Ag/Pd (above) and DP 5744-Au co-fired samples.

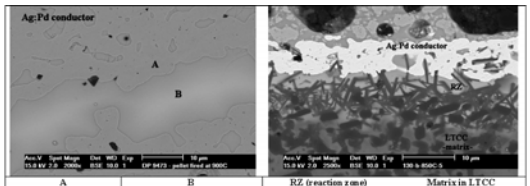

A		B		RZ (reaction zone)		Matrix in LTCC	
Element	Atomic %	Element	Atomic %	Element	Atomic %	Element	Atomic %
Ag	76	O	57	O	59	O	55
Pd	24	Zn	10	Na	4	Al	10
		Al	4	Al	10	Si	26
		Si	8	Si	15	Pb	2
		Bi	18	Pb	4	Ca	3
		Others	3	Bi	6	Na	2
				Others	2	Others	2

Figure 8. EDXS analysis of the reaction zone (RZ), located between the conductor and the LTCC.

The reaction zone, which is observed in a different contrast, is located between the LTCC substrate and the Ag/Pd conductor. An understanding of this region can well be based on the interaction of the glass phases of the LTCC substrate and the conductor, which clearly influences the properties. The extent and the nature of this interaction is best seen in figure 8, which shows the EDXS analysis of the Ag/Pd pellet, LTCC and the reaction zone. According to the EDXS results, the reaction zone contains high amount of Bi that can only originate from the conductor. In a similar manner, Pb (originally absent in the conductor) is found in the close neighborhood of it. On the other hand, the sample co-fired with the Au conductor does not exhibit a reaction zone and the conductor line is not significantly altered by any kind of penetration or diffusion.

Therefore, the relation obtained in the TCR/SR versus resistor length analysis (figure 4), which demonstrated a less favorable result for the Ag/Pd conductor, is explained using the SEM and EDXS. It is observed that the glass content of the Ag/Pd conductor reacted strongly with that of the LTCC, which accordingly influenced the electrical properties.

3. Cavity formation in buried samples

As explained previously, physical issues arise mainly from the shrinkage mismatch of the tape and the thick-film pastes[28-29], which finally destroy the fired structure at different extents. However, another defect, which turned out to be the major causes for the unreliable electrical properties presented in the previous part, was observed: swelling inside the buried structures (Figure 9), which forms cavities at the conductor-resistor intersection. Interestingly, cavity formation only occurs in samples with buried Au conductors (both) and not with the Ag/Pd.

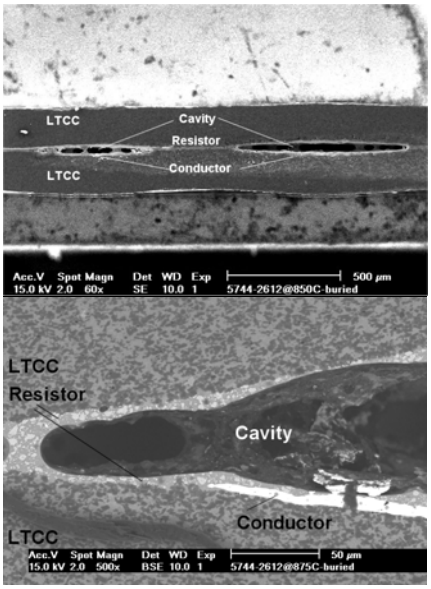

Figure 9. Cavities in the DP 5744 buried sample.

Although the exact source is still being examined, our observations indicate that cavity formation is either due to a high temperature oxidation-reduction reaction or organics burnt-out as a result of which gas evolution occurs. However, in this case, degassing is evidently not completed before the close-up of the porosity in the LTCC surface. In order to check the porosity elimination temperature of the LTCC surface, we built up a system, which is shown in figure 10. The paper does not intend to describe its functioning or the measurements in details. However it is based on the relaxation time measurement of the pressure drop through the porous LTCC substrate between the O-rings.

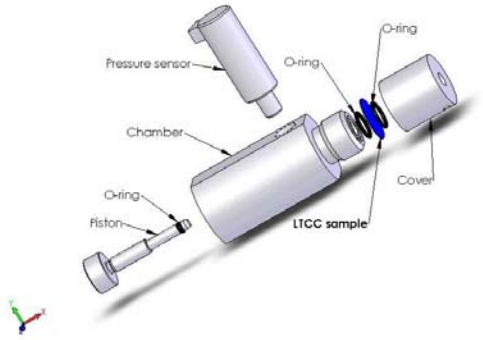

Figure 10. Closed chamber for determination of porosity elimination temperature.

The results are presented in figure 11, which shows the pressure drop in the LTCC surfaces fired at different temperatures. It is seen that the porosity is eliminated approximately at 785°C. Thus any reaction that leads to gas liberation (reduction, organic burn-out, etc…) after this temperature increases the gas pressure between the LTCC sheets of the buried sample and deforms the structure.

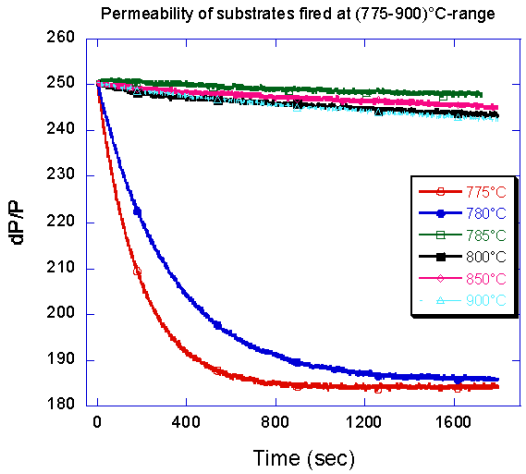

Figure 11. Qualitative detection of the porosity elimination temperature. Linear pressure drop represents the porosity-free substrates.

To check the validity of this statement, we fired buried samples with Au (DP 5744) conductor at different temperatures. A series of SEM images, which shows the corresponding structures, is shown in figure 12.

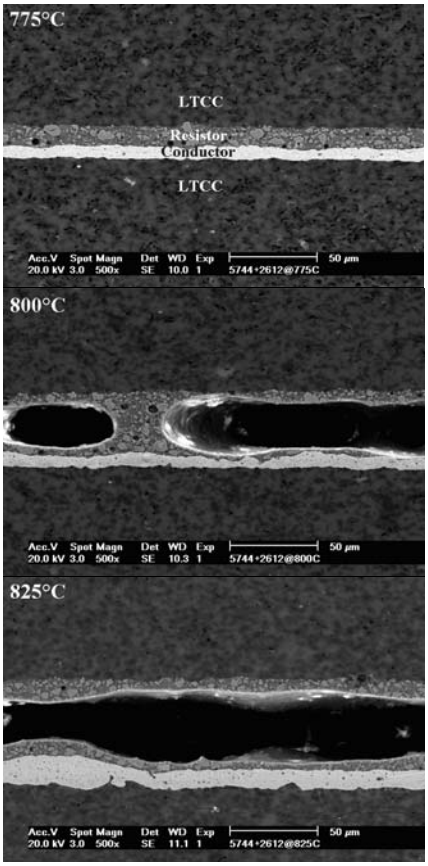

Figure12. Extent of deformation in buried samples, fired at different temperatures.

According to our current understanding, the formation of the gas, which probably arises from elemental interaction after 785°C or reduction of an oxide, is estimated to cause the observed effects shown in figures 9 and 12. Another interesting result is that the samples buried with Ag/Pd conductors did not show this type of deformation at resistor-conductor contact.

In order to better understand the origin of this deformation, we buried the individual pastes by screen-printing them on LTCC sheets. Upon firing we observed that only ESL 2612 resistor paste resulted in swelling-type deformation and neither Au nor the Ag/Pd conductors alone deformed the buried structure. Thus, the Ag/Pd conductor apparently suppresses the occurrence of swelling, through the large amount of chemical interaction it exhibits. However, the exact mechanism of cavity formation and suppression thereof remains unknown.

4. A preliminary study to reduce the differential shrinkage-related deformation

Differential shrinkage between the components of an LTCC module is, to a greatest extent, the origin of deformation such as warpage, curling, etc (figure 13). This is an undesired consequence from both application point of view (membranes, channels, etc…) and scientific interest. Thus, in this section we propose a method to match the shrinkage rates of the tape and the conductor to end up with reduced deformation.

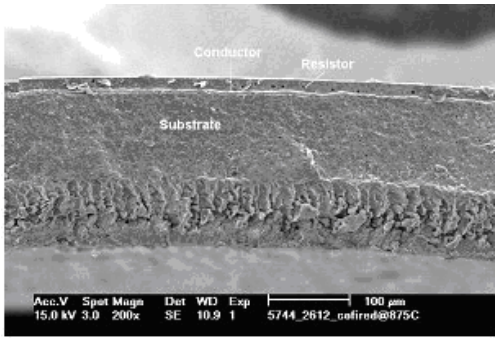

Figure 13. Warpage on the LTCC tape due to unmatched shrinkage between the conductor and the LTCC tape.

In order to match the shrinkage behavior of the conductor to that of the LTCC tape, we basically mixed the commercial conductors - DP 9473 Ag/Pd used in this study and ESL 9562 Ag/Pd/Pt – with the selected dopants. The exact description of the used materials is presented in table 2. Mixture was prepared according to 10 or 20% of additive (prepared from SiO_s powder – commercial- and LTCC tape according to the method described previously) to paste ratio by weight, which was followed by homogenization in the three-roll mill. The prepared paste was then partially dried to make the dilatometry analysis and partially screen-printed on the LTCC sheets for co-firing with the PTC resistor used in this study.

Table 2. Materials used for modification of pastes

Paste	Specification	Additive	
		SiO_2*	LTCC
DP 9473	Ag/Pd	10%	10%
		20%	20%
ESL 9562**	Ag/Pd/Pt	10%	10%
		20%	20%

**SiO_2: Sihelco, Sikron B 600*
*** Fritless conductor with Cu additions(Ag/Pd~16)*

The results of the dilatometry analysis, being the method used for figure of merit – shrinkage, are presented in figure 14. It is seen in both graphs that the additives play different roles on the shrinkage behavior of the pastes. For instance addition of LTCC powder, which was aimed to establish a shrinkage behavior similar to that of the tape, results in expansion starting from 700°C. On the other hand addition of SiO_s, which is known to increase the glass transition temperature by promoting network formation[27], leads to a shrinkage behavior that is similar to the tape.

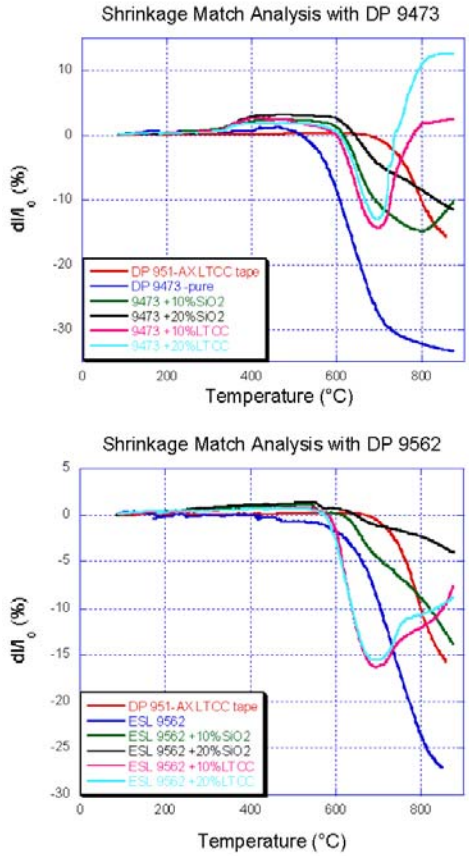

Figure 14. Dilatometry analysis for the doped pastes.

The effects of the more favorable additive -SiO_2 is presented in table 3, which is derived from figure 14. One can see that the onset temperature of the paste shrinkage can be pushed up to that of the LTCC tape effectively. In case of the doped DP 9473 paste, this is seen as a considerable change both in the total value of temperature shifted and the amount of shrinkage.

Table 3. Effect of SiO_2 addition on pastes

Paste (ratio of doping)	$T_{shr.}^{+}$ (°C)	%Shrinkage^{++} (-)
DP 9473	516	23
DP 9473 + 10%	618	7.7
DP 9473 + 20%	644	2.3
ESL 9562	430	5.5
ESL 9562 + 10%	615	3
ESL 9562 + 20%	646	0.7

$T_{shr.}^{+}$:Onset temperature of shrinkage of the paste($\Delta l/l<0$)
%Shrinkage^{++}: Amount of paste shrinkage at the onset temperature of the tape shrinkage (670°C).

Thus, we prepared new samples by screen-printing the commercial DP 9473, its doped versions with 20% SiO_2 and 10% LTCC on the tapes and checked the deformation on the surface of the co-fired samples (figure 15). We used the LTCC powder-added paste in order to check the final deformation on the structure, although its dilatometry data follows a different trend.

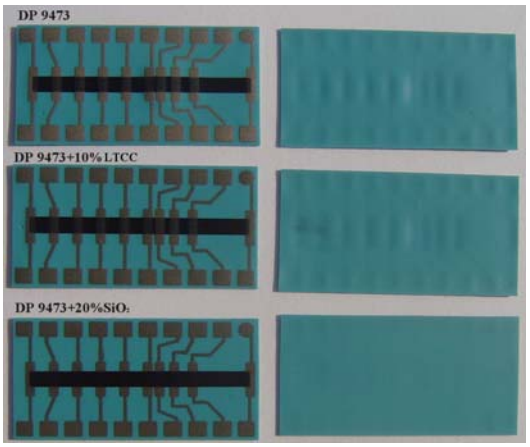

Figure 15. Pure (first row) and doped DP 9473 pastes co-fired on the LTCC tapes. Column on the right hand side shows the back-sides of the samples.

It is clearly seen that doping with 20%SiO_2 addition yielded almost no deformation on the tape. Moreover firing this paste on 114μ-thick LTCC tape (Du Pont 951-AT) also resulted in limited deformation on the tape.

Following this result, we made SEM analysis to see the effects of doping on the microstructure. Figure 16 and 17 demonstrates the comparison of the microstructures of the undoped and 20% SiO_2-doped DP 9473 pellets and tape-conductor-resistor interface respectively.

In figure 16, the effect of SiO_2 powder addition can be observed clearly by the modified microstructure. They are the black particles, which are homogeneously dispersed in the matrix (Ag/Pd seen in white) in different size and morphology. Consequently the glass phase, which is seen as grey contrast, is more localized. Although it is an early estimate, the addition of SiO_2 particles seems to suppress the mobility of the glass phase by pinning it. According to our understanding this is the mechanism, which stabilizes the glass and reduces the corresponding deformation.

In figure 17, on the other hand, it is remarkable that the conductor line in the doped (second image) version is mostly discontinuous. This is observed to be due to the SiO_2, which is seen as longitudinal black particles located in the conductor line (large, black circles in the resistor are pores).

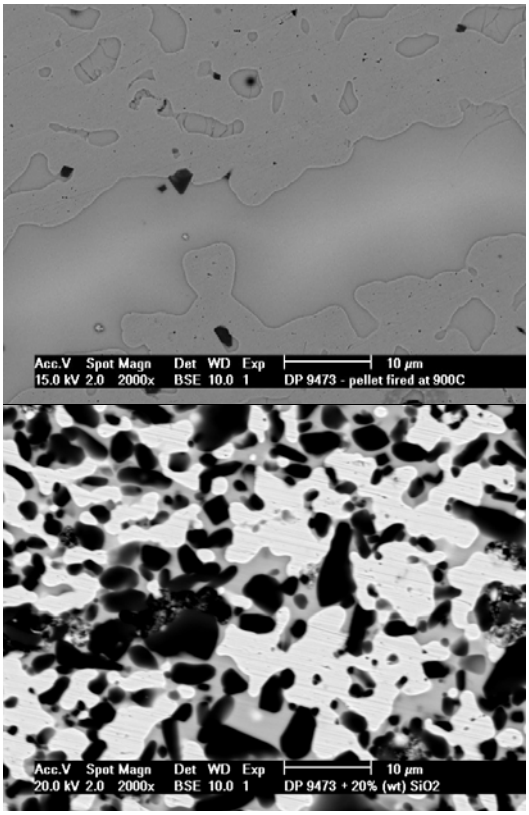

Figure 16. Pure (first) and 20% (wt) SiO_2 doped DP 9473 pellets. The microstructure changes upon addition of SiO_2.

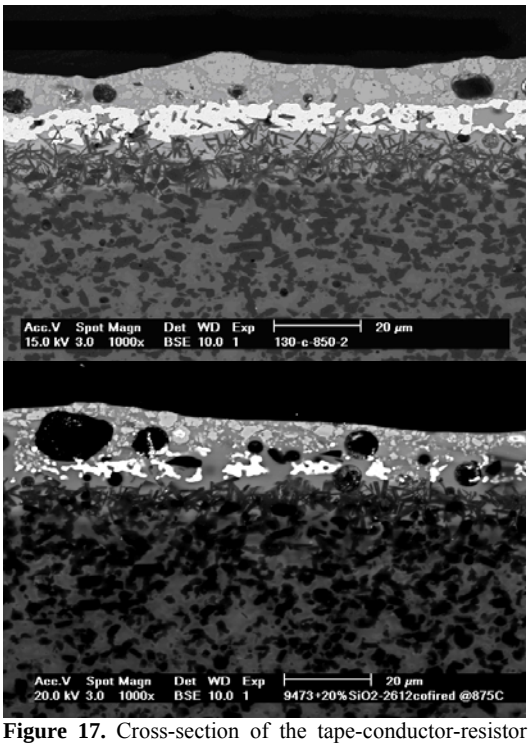

Figure 17. Cross-section of the tape-conductor-resistor interface co-fired. Pure (first) and 20% SiO_2-doped DP 9473 conductors.

We finally checked the electrical properties of the new pastes with 20% SiO_2 and 10% LTCC. The TCR and SR values of the pastes those co-fired at 875°C are shown in figure 18.

The influence of SiO_2 and LTCC powder addition is directly observed as an increase of SR. It is evident that these species increase the resistance considerably -by a factor of 2. However the value of TCR can not be considered deviated from that of the undoped paste. It is interesting that the doped pastes reach a SR value that is expected for the undoped paste by specification.

Conclusions

This paper summarizes the influence of processing conditions on the properties of the selected thick-film compositions, particularly PTC resistors. The results are grouped as chemical and physical issues, which are discussed according to the important observations made.

The chemical issues are classified as those, which are provoked by the glass content of the thick-film composition. It is shown in details that the composition and the quantity of the glass phase in the selected thick-film paste is prone to chemical interactions with the surroundings, the extent of which can alter the final electrical properties.

Deformations such as warpage, swollen buried structures are treated in the physical issues section. Although the origin of swelling is yet being studied, it is attributed to the imprisoned burnout products of the pastes in the buried LTCC upon porosity elimination around 785°C. The latter defect on the other hand, stems from the densification of the thick-film pastes much prior to the tape and thus deforming the whole structure. A method is proposed with the aim of overcoming this problem, which is based on doping the paste. The results show that the selected additive yields satisfactory results both in physical and electrical properties, by almost eliminating the deformation on the tape and not altering the value of TCR considerably.

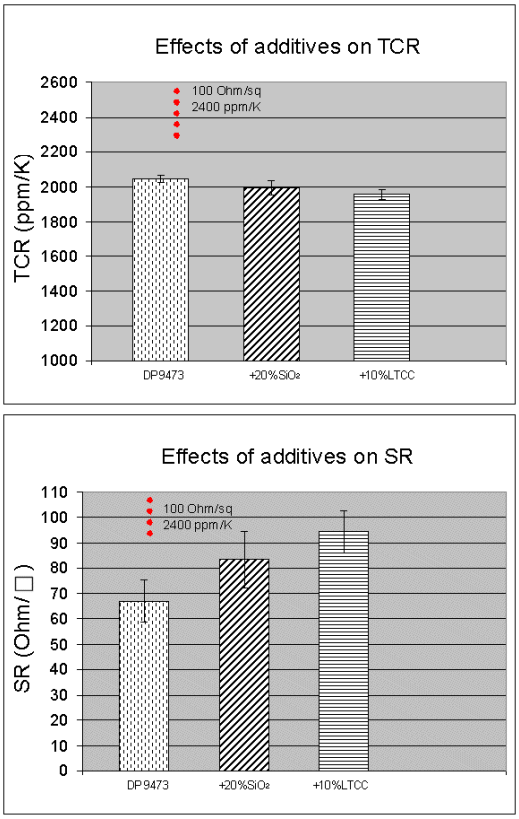

Figure 18. Effect of additives on TCR (above) and SR of PTC resistor.

References

[1] S. Annas, "Advances in low temperature co-fired ceramic (LTCC) for ever increasing microelectronic applications", 2003 IEEE Electronic Components and Technology Conference, pp. 1691-1693, 2003.

[2] T. Thelemann, H. Thust and M. Hintz, "Using LTCC for Microsystems", Microelectrocnics International, 19, pp. 19-23, 2002.

[3] R. Kulka, M. Mittweger, P. Uhlig, C. Günther, "LTCC-multilayer ceramic for wireless and sensor applications", IMST GmbH, http://www.ltcc.de, 2001.

[4] M.G-Rubio, L.M.S-Laguna, P.E-Vallejos and J.J.S-Aviles, "Overview of LTCC tape technology for meso-system technology (MsST), Sensor. Actuat. A-Phys, 89, pp. 222-241, 2001.

[5] J. Kita, A. Dziedzic, L.J.Golonka and A. Bochenek, "Properties of laser cut LTCC heaters", Microelectron. Reliab., 40, pp. 1005-1010, 2000.

[6] R.L.Brown, A.A.Shapiro, P.W. Polinski, "The integration of passive components into MCMs using advanced LTCC", Int. J. Micro. Elec. Pack., 16, pp. 328-338, 1993.

[7] R.R. Tummala, "Ceramic and glass-ceramic packaging in the 1990s", J. Am. Ceram. Soc., 74, pp. 895-908, 1991.

[8] R.L. Brown, W.R. Dick Smith, “Embedded passive functions for RF and mixed-signal circuits”, National Semiconductor Corporation – Internal report.

[9] J.J.S-Aviles and P.E-Vallejos, “Medical device manufacturing and technology- Processing of materials for biomedical applications, Report, Electrical Engineering, University of Pennsylvania.

[10] T. Maeder, H. Birol, C. Jacq and P. Ryser, "Integrated Microfluidic Devices Based on Low-Temperature Co-Fired Ceramic (LTCC) Technology", Proceedings, 4th Korea-Switzerland Joint Symposium, Materials and MEMS for Life Science Applications, Les Diablerets, 2004.

[11] H. Birol, T. Maeder, C. Jacq and P. Ryser, "3-D structuration of LTCC for Sensor Micro-fluidic Applications", Proceedings, 3rd European Microelectronics and Packaging Symposium, Prague, pp. 366-371, 2004.

[12] M.G-Rubio, L.S.-Laguna, M. Smith and J.J.S.-Aviles, “LTCC technology multilayer Eddy-current proximity sensor for harsh environments”, International Symposium on Microelectronics, pp. 676-681, 1999.

[13] M.G-Rubio, L.M.S-Laguna, P.J. Moffett and J.J.S-Aviles, “The utilization of LTCC-ML technology for meso-scale EMS, a simple thermistor based flow sensor”, Sensor Actuat, 73, pp. 215-221, 1999.

[14] H. Lynch, J.Park, P.A.E-Valejos, J.J. S-Aviles and L.S-Laguna, “Meso-scale pressure transducers utilizing LTCC tapes”, Materials Research Society Symposium Proceedings, 546, pp. 177-182, 1999.

[15] H.Teterycz, L.J.Golonka, J.Kita, R.Bauer, B.W. Licznerski, K. Nitsch and K. Wisniewski, “New design of an SnO_2 gas Sensor on LTCC”, Sensor Actuat B-Chem, 47, pp. 100-103, 1998.

[16] L.J.Golonka, B.W. Licznerski, K. Nitsch, H. Teterycz, R. Bauer, K.J. Wolter, “Examples of gas sensors by application of thick-film technology”, Proc. 43rd Int. Sci. Colloq., TU Ilmenau, pp. 465-470, 1998.

[17] M.A. Fonseca, J.M. English, M. von Arx and M.G.Allen “High-temperature characterization of ceramic pressure sensors”, Georgia Institute of Technology, School of Electrical and Computer Engineering.

[18] M. Jackson, M. Pecht, S.B. Lee and P. Sandborn, “Integral, Embedded, and Buried Passive Technologies”, Calce Electronic Systems and Products Center, 2003.

[19] G.E. Pike and C.H.Seager, “Electrical properties and conduction mechanisms of Ru-based thick-film (cermet) resistors” Journal of Applied Physics, Vol.48 (12), pp. 5152-5169, 1977.

[20] C.J. Ting, C.S. His and H.Y. Lu, “Interactions between ruthenia-based resistors and corderite-glass substrates in low-temperature co-fired ceramics”, J. Amer. Ceram. Soc., 83 (12), pp. 2945-2953, 2000.

[21] P.Yang, M.A.Rodriguez, P.Kotula, B.K.Miera and D.Dimos, “Processing, microstructure and electric properties of buried resistors in low-temperature co-fired ceramics”, J. Appl. Phys., 89 (7), pp. 4175-4182, 2001.

[22] C.S.Hsi and M.W.Lee, “Properties of ruthenia-based resistors embedded in low-temperature co-firable ceramic substrates”, Jap. Journal Appl. Phys., 41 (8), pp. 5323-5328, 2002.

[23] H. Birol, T. Maeder, C. Jacq and P. Ryser,, "Effects of firing conditions on thick-film PTC thermistor characteristics in LTCC technology", Proceedings, IMAPS Conference on Ceramic Interconnect Technology, Denver, pp. 106-109, 2004.

[24] H. Birol, T. Maeder, C. Jacq and P. Ryser, “Investigation of interactions between co-fired LTCC components”, Electroceramics IX, Cherbourg, accepted for publication in the special issue of the Journal of the European Ceramics Society, 2004.

[25] H. Birol, T. Maeder, C. Jacq and P. Ryser, "Processing – Property Relationship in Co-fired LTCC Structures", Third International Conference on Microwave Materials and Their Applications, Inuyama, accepted for publication in the special issue of the Journal of the European Ceramics Society, 2004.

[26] K. Pitt, “Handbook of thick-film technology”, Electrochemical Publications, second edition, , Bristol, Chapter 8, pp.181-209, 2005.

[27] R.C. Sutterling, G.O. Dayton and J.V.Biggers “Thick-film resistor/dielectric interactions in a LTCC package”, IEEE Trans. Comp. Pack. Manuf. Tech., 18, Part B, pp. 346-351, 1995.

[28] T. J. Garino, “The co-sintering of LTCC materials”, Ceramic Interconnect Technology Conference, pp. 171-176, 2003.

[29] G.Q. Lu, R.C. Sutterlin and T.K. Gupta, “Effect of mismatched sintering kinetics on camber in a low-temperature cofired ceramic package”, J. Amer. Ceram. Soc., 76 (8), pp.1907-1914, 1993.